ARCHIVES OF BIOCHEMISTRY AND BIOPHYSICS
Vol. 301, No. 1, February 15, pp. 71–76, 1993

Structural Heterogeneity of Caucasian *N*-Acetyltransferase at the NAT1 Gene Locus[1]

Kostas P. Vatsis[2] and Wendell W. Weber
Department of Pharmacology, Medical School, The University of Michigan, Ann Arbor, Michigan 48109-0626

Received August 31, 1992, and in revised form October 19, 1992

The human N-acetylation polymorphism is a genetic trait phenotypically reflected by differences in *N*-acetyltransferase (NAT) activity with therapeutic agents (rapid and slow acetylation), but a genetic invariability in N-acetylation of some arylamine drugs is also known. There are two highly similar human NAT genes: *NAT1* is thought to encode a genetically invariant protein, whereas *NAT2* has conclusively been shown to represent a polymorphic locus. This study demonstrates the presence of discrete *NAT1* structural variants among Caucasians. These were detected by direct sequencing of 1.6-kilobase *NAT1* fragments generated by the polymerase chain reaction with liver and leukocyte DNA from 13 subjects of established acetylator phenotype and *NAT2* genotype. A prominent alteration in one of the variants was obliteration of the consensus polyadenylation signal (AATAAA→AAAAAA). Several mutations were discernible in all regions of the second variant allele, including silent (codon 153) and nonsilent (Ser-214→Ala) substitutions in the coding region and deletion of nine bases from an AT-rich segment in the 3′ untranslated region. One-half of the unrelated subjects were either homozygous or heterozygous for the mutant *NAT1* alleles, both of which obeyed a Mendelian inheritance pattern. These novel results unambiguously show that human *NAT1*, like *NAT2*, is a polymorphic locus. © 1993 Academic Press, Inc.

The N-acetylation polymorphism is an inherited trait demonstrable in human populations by polymodal frequency distribution histograms for the elimination of pharmacologically diverse therapeutic agents *in vivo*, as well as by catalytic activity differences in hepatic and extrahepatic cytosolic N-acetylation of these substances *in vitro*. Such differences distinguish phenotypically rapid from slow acetylators. On the other hand, unimodal frequency distribution histograms have been obtained for the metabolism of *p*-aminosalicylic acid and sulfanilamide by rapid and slow acetylators of isoniazid, a phenomenon referred to as monomorphic (genetically invariant) acetylation. Of toxicological interest is the additional involvement of cytosolic NATs[3] (acetyl-CoA:arylamine *N*-acetyltransferase, EC 2.3.1.5) in the bioactivation of environmental carcinogens (1, 2).

Two human NAT cDNAs (3) and genes (4, 5) [*NAT1* and *NAT2* (4)] were shown to encode highly similar proteins with overlapping substrate specificities, and several lines of evidence suggested that NAT1 and NAT2 represented the monomorphic and polymorphic proteins, respectively (3, 4, 6). Structural variants of *NAT2* with coding region and far downstream mutations were subsequently identified in Japanese and Caucasian slow acetylators of sulfamethazine, caffeine, dapsone, and isoniazid (3, 5, 7–9). Mammalian cell culture expression systems revealed that the mutant *NAT2* alleles did not affect mRNA steady-state levels but caused parallel decreases in the cytosolic content of immunoreactive NAT2 and in N-acetylation activities (3, 9). These findings were in accord with those obtained with hepatic tissue from phenotypically slow acetylators with mutant *NAT2* genotypes (9), thereby establishing that *NAT2* is a polymorphic gene locus. Unlike these strides with *NAT2*, however, a sys-

[1] This work was supported by Grant GM-44965 from the National Institutes of Health.

[2] To whom correspondence should be addressed at Department of Pharmacology, M6322/0626 Medical Science I, Medical School, The University of Michigan, Ann Arbor, MI 48109-0626. Fax: (313) 743-4450.

[3] Abbreviations: N-acetyltransferase proteins and genes are depicted in regular type (NAT) and italics (*NAT*), respectively; PCR, polymerase chain reaction; WBC(s), white blood cell(s); UTR, untranslated region; IP(s), internal (sequencing) primer(s); 'wt', 'wild-type'; bp, base pair(s); kb, kilobase(s); nt, nucleotide(s); RFLP, restriction fragment length polymorphism; PABP, poly(A) binding protein.

0003-9861/93 $5.00

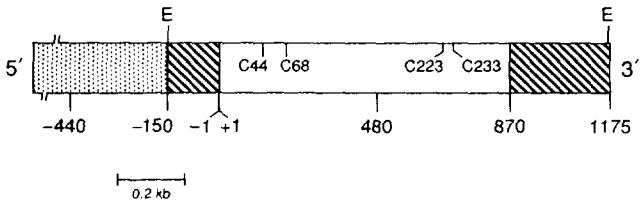

FIG. 1. Structure of human *NAT1*. The location of the 5′ UTR has been defined by NAT cDNAs (3, 5), but the actual transcriptional start site(s) have not been mapped. The four cysteines conserved in human *NAT1* and *NAT2* (3–5) are shown in the coding exon (open bar). Stippled bar, 5′ flank; hatched bars, 5′ and 3′ UTR. E, *Eco*RI.

tematic survey of *NAT1* genotypes has not been undertaken to date.

The present study is the first report on the existence of human *NAT1* variant alleles, identified by direct sequencing of a 1.6-kb fragment of PCR-generated *NAT1* with liver and leukocyte DNA from 13 individuals (three of whom were family members) of defined acetylator phenotype and *NAT2* genotype. The most striking change in one of the *NAT1* variants was obliteration of the highly conserved polyadenylation signal (AATAAA→AAAAAA). Different mutational events took

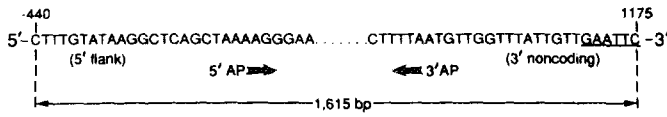

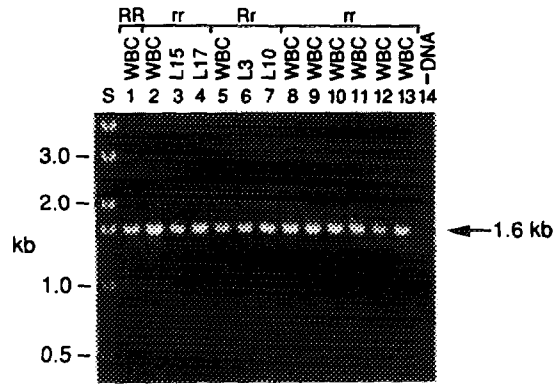

FIG. 2. Amplification and identification of *NAT1*. (Upper) Amplification primers 5′ AP (sense; positions −440 to −413) and 3′ AP (antisense; complementary to nt 1148–1175) were mixed with genomic DNA and *Taq* DNA polymerase, and allowed to undergo 30 PCR cycles (8). (Lower) Aliquots (10 μl) of PCR mixtures were submitted to electrophoresis on 1% agarose gels and the products were visualized by ethidium bromide staining. Mixtures with liver DNA were loaded in lanes 3, 4, 6, and 7, and those with leukocyte DNA in the lanes marked WBC. Template DNA was omitted from the mixture in lane 14. Standard (1 μg of 1-kb ladder; BRL) was added to the lane marked S. Acetylator phenotypes: RR, homozygous rapid; rr, homozygous slow; and Rr, heterozygous.

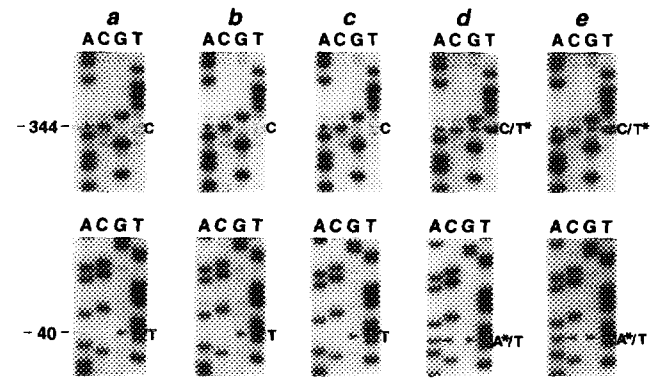

FIG. 3. Autoradiograms of 5′ flanking (upper) and 5′ UTR (lower) segments. The sequences in columns a–e were obtained with the following samples depicted in Fig. 2: a, samples (lanes) 1, 3, 4, 5, 10, and 11; b, sample 8; c, samples 6 and 7; d, sample 9; and e, samples 2, 12, and 13. (Upper) The segment was sequenced with sense primer IP1 located at *NAT1* positions −408 to −392 (5′-AGTGGGTCAGGTACCAC-3′). Electrophoresis was carried out with 7% polyacrylamide/8 M urea gels. (Lower) The sequences were determined with antisense primer IP2 (complementary to nt 89–105; 5′-AACAGCTCGGATCTGGT-3′). Asterisks indicate the bases that differ from those of *NAT1* in column a. Heterozygosities are characterized by duplicate comigrating bands.

place in the second variant, including silent and nonsilent (Ser-214→Ala) point mutations in the coding region and a sizeable 9-bp deletion (10) from an AT-rich segment in the 3′ UTR. The mutant *NAT1* alleles were present in 50% of the subjects, and displayed Mendelian inheritance characteristics.

EXPERIMENTAL PROCEDURES

DNA isolation and determination of acetylator status. Genomic DNA was available from seven subjects of established acetylator phenotype

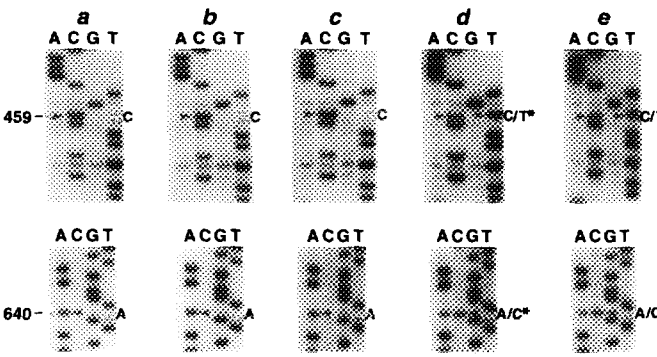

FIG. 4. Autoradiograms of coding region segments. The sequences in columns a–e were displayed by the *NAT1* samples enumerated in Fig. 3. The segments were sequenced with antisense primers IP3 [complementary to nt 532–547; 5′-CTTCTAGGAGATCAGA-3′ (upper)] and IP4 [complementary to nt 716–732; 5′-GAATCTCCTATGGGTGA-3′ (lower)]. Nucleotides differing from those of *NAT1* in column a are marked with an asterisk.

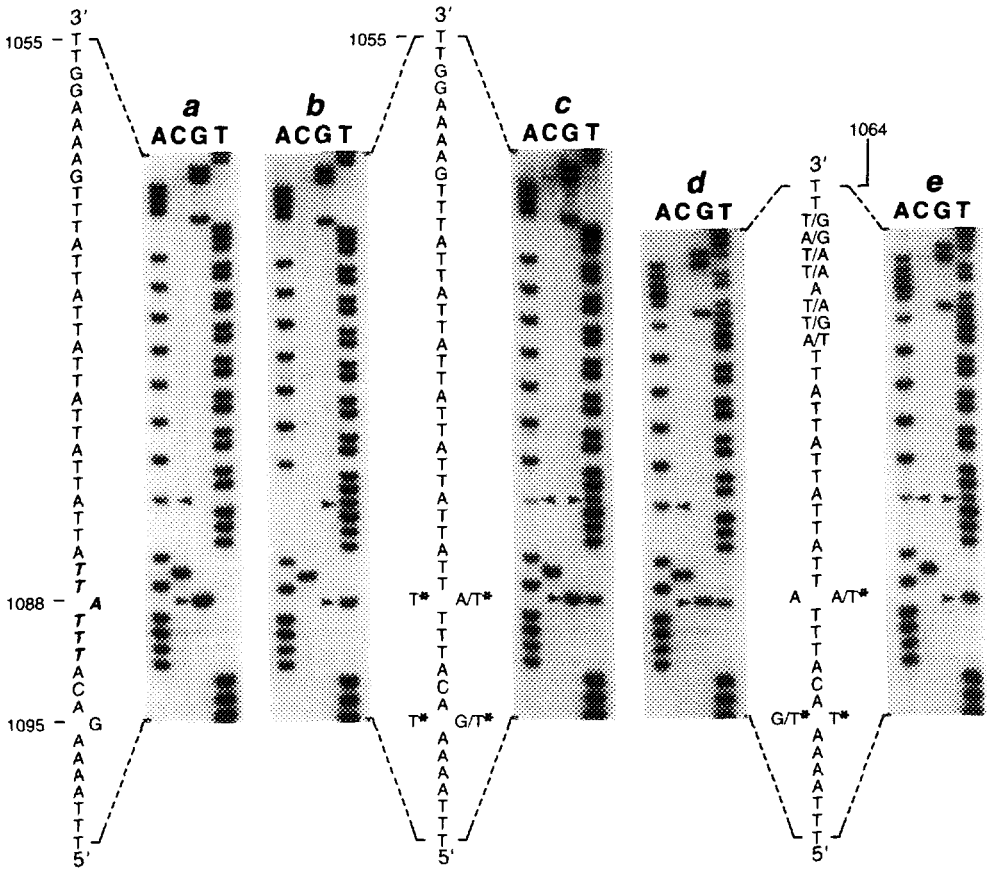

FIG. 5. Autoradiogram of a 3′ UTR segment spanning the polyadenylation signal. The sequences in columns a–e were obtained with the samples listed in Fig. 3, and were determined with antisense primer IP5 (complementary to nt 1129–1144; 5′-TCTAGCATAAATCACC-3′); samples were submitted to electrophoresis on 7.5% polyacrylamide/8 M urea gels. The polyadenylation signal (nt 1086–1091) is shown in bold letters. The duplicate bands toward the top of the sequences in columns d and e are the result of a 9-bp deletion from one of the alleles of these heterozygotes. The deletion occurred in the segment extending from nt 1065 to 1090; the exact deletion site is unknown, but the mutant sequences are the same regardless of the location of the deleted nonanucleotide.

and *NAT2* genotype (8), and was also extracted (11) from WBCs from six additional healthy volunteers phenotyped as indicated in Table I.

Oligonucleotides. *NAT1* amplification primers (see Fig. 2) were made with *Bam*HI and *Sst*I linkers and a GC pair attached at the linker ends (total length, 36 nt). Double-stranded sequencing of *NAT1* was performed with a total of eight internal (sequencing) primers (IPs), which are not shown here since the gene sequence has been published (4). Mutation sites were verified with at least two IPs in opposite orientations; the sequence and gene location of five of these IPs are given in the appropriate figure legend. End-labeling of IPs was carried out with [γ-^{32}P]ATP, and radiolabeled oligonucleotides were purified by gel filtration chromatography (8).

PCR amplifications and direct sequencing. The composition of PCR mixtures (with amplification primers at 0.5 μM for *NAT1* and 0.25 μM for *NAT2*) and amplification conditions have been reported (8). Direct sequencing of PCR-generated *NAT1* and *NAT2* was as before (8), except that 5′-^{32}P-labeled IPs were included at 10^6 cpm and the annealing temperature was at the T_m for the particular primer. Samples were submitted to electrophoresis on 6% polyacrylamide/8 M urea gels, except where indicated otherwise.

RESULTS

The protein-coding region and 5′ UTR of *NAT1* are uninterrupted by introns (Fig. 1), whereas only the coding exon of *NAT2* is free of intervening introns (3–5). Amplification of *NAT1* by PCR (Fig. 2, upper) led to formation of a single DNA band of the expected size (1.6 kb) (Fig. 2, lower, lanes 1–13); no bands were generated in the absence of DNA (lane 14). Both strands of the entire 1.6-kb *NAT1* fragment from the 13 individuals were sequenced directly. The normal or 'wt' sequence was found to be identical to that determined by single-stranded sequencing of *NAT1* from a heterozygote (4), except that a C instead of an A was invariably present at position 1095 in the 3′ UTR. This is also true for the gene and corresponding cDNA from Japanese (3, 5).

The 'wt' *NAT1* sequence is depicted in column a of Figs. 3–5. The upstream (Fig. 3) and coding region (Fig. 4) segments of the *NAT1* samples in columns b and c were devoid of mutations, whereas the samples in columns d and e exhibited heterozygosities in the 5′ flanking region (nt −344; Fig. 3, upper), 5′ UTR (nt −40; Fig. 3, lower), and at positions 459 (Fig. 4, upper) and 640 (Fig. 4, lower) in the coding region. Figure 5 illustrates 3′ UTR mutations

TABLE I

Caucasian *NAT1* and *NAT2* Genotypes Ascertained from Direct DNA Sequencing

		NAT1 sequence									
		5'Flank/ 5' UTR		Protein-coding region		3' Untranslated region				Genotype designation	
Sample/ subject[a]	N-acetylation phenotype[b]	nt −344	nt −40	Codon 153[c]	Codon 214	Positions 1065–1090[d]	Polyadenylation signal[e]	nt 1088[f]	nt 1095[f]	*NAT1*[g]	*NAT2*[h]
1, 5, 10, 11 3, 4	RR, Rr, rr, rr rr, rr	C	A	ACG (Thr)	TCA (Ser)	Intact	Normal AATAAA	T	C	V_1V_1	R_1R_1, R_1r_3, r_2r_2, r_2r_3 r_3r_3, R_1r_3
8	rr	C	A	ACG (Thr)	TCA (Ser)	Intact	Mutated AAAAAA	A	A	v_2v_2	r_2r_3
6, 7	Rr, Rr	C	A	ACG (Thr)	TCA (Ser)	Intact	$AA\overset{T}{A}AAA$	T A	C A	V_1v_2	R_1R_1, r_2r_3
9	rr	C T	A T	$AC\overset{G}{A}$ (Thr)	$\overset{T}{G}CA$ (Ser/Ala)	9-Base deletion	$AATAA\overset{A}{T}$	T	C A	V_1v_3	r_2r_3
2, 12, 13	rr, rr, rr	C T	A T	$AC\overset{G}{A}$ (Thr)	$\overset{T}{G}CA$ (Ser/Ala)	9-Base deletion	$AATAA\overset{A}{T}$	A T	A	v_2v_3	r_2r_2, r_2r_2, r_2r_3

[a] Subjects 2, 8, and 9 are members of a two-generation family.

[b] Phenotyping methods and N-acetylation activities for individuals 1–7 have been reported (8). Urinary caffeine metabolite ratios of 1.1 and 0.9 were determined for persons 8 and 9, respectively [a ratio of 1.82 separates slow from rapid acetylators (12)]. The acetylator phenotype of individuals 10, 12, and 13 was assessed with sulfamethazine *in vivo*, and the amount of N-acetylated metabolite detected in the urine 4.5 h after drug administration (expressed as % of total) was 40.9, 37.1, and 57.0%, respectively [the antimode for this method is ~72% (13)]. A ratio of 0.11 was obtained for N-acetylated to unmetabolized dapsone in serum from subjects 11 and 13 [the antimode is 0.26 (12)].

[c] Codon 153 lies within an inverted repeat with termini at nt 446 and 464. In addition to the mutated G^{459}, *NAT1* from the deletion variants contained comigrating bands at five of the eight juxtaposed positions on the palindrome stem but only in opposite orientations [nt 460–464 (5' → 3') and 450–446 (3' → 5')], suggesting that the duplicate bands at these positions may not be real heterozygosities; definitive proof will be required before this possibility can be ruled out.

[d] The intact and deleted sequences were shown in Fig. 5 and are illustrated schematically in Fig. 6.

[e] The normal or mutated polyadenylation signal occupies positions 1086–1091 in the 'wt' and nondeletion variant *NAT1*, but is shifted 9 bp upstream (nt 1077–1082) in *NAT1* from the deletion variants.

[f] When gaps are inserted in the deletion variant allele, the sequence from nt 1096 to 1104 is identical to that of the 'wt' and nondeletion variant *NAT1* alleles, i.e., TTTTAAAGA.

[g] *NAT1* genotype designations are informal; both letters and numbers were arbitrarily assigned to the 'wt' (V_1) and two allelic variants (v_2 and v_3).

[h] The genotypes of subjects 1–7 have been published (8). PCR-generated *NAT2* (8) with DNA from subjects 8–13 was sequenced directly from a position 100 nt 5' of the initiator ATG codon to the end of the 3' UTR (nt 1169); the sequences were determined with the IPs reported previously (8) and an additional IP located near the 3' end of the coding region (nt 844–860; 5'-AAACCTGGTGATGGATC-3'). No mutations were seen in the 3' UTR of *NAT2* from these slow acetylators.

entailing A→T and G→T transversions at nt 1088 and 1095, respectively (column b), heterozygosities at one or both of these positions (columns c and d), comigrating bands at nt 1088 and a G→T substitution at nt 1095 (column e), as well as a 9-bp deletion from the segment extending from nt 1065 to 1090 (columns d and e). The presence of identical iterative triplet motifs within this segment precluded ascertainment of the precise location of the deletion site (see also Fig. 6).

A summary of the foregoing and a comparison of acetylator phenotypes with *NAT1* and *NAT2* genotypes are presented in Table I. The altered polyadenylation signal in variant v_2v_2 was most conspicuous. A homozygote of variant allele v_3 was not found, suggesting that genotype v_3v_3 may occur rather infrequently. In contrast, all three possible allelic combinations were detected (V_1v_2, V_1v_3, and v_2v_3). It is evident from heterozygote V_1v_3 and compound heterozygotes v_2v_3 that a number of mutations (representing different mutational events) segregated with allele v_3, the more salient of which were silent and nonsilent (Ser-214→Ala) substitutions in the coding region, and deletion of a nonanucleotide from the 3' UTR. Overall, five of six possible *NAT1* genotypes were identified with a relatively small sample size, arguing for the prevalence of the observed mutations among Caucasians. Regarding *NAT2*, the genotypes [two r_2r_2 and four r_2r_3] determined for the six previously unreported samples (Nos. 8–13) were in perfect agreement with the acetylator phenotype (rr) of the persons from whom they originated.

DISCUSSION

The results of this investigation offer lucid evidence that the Caucasian NAT1 gene locus, hitherto described

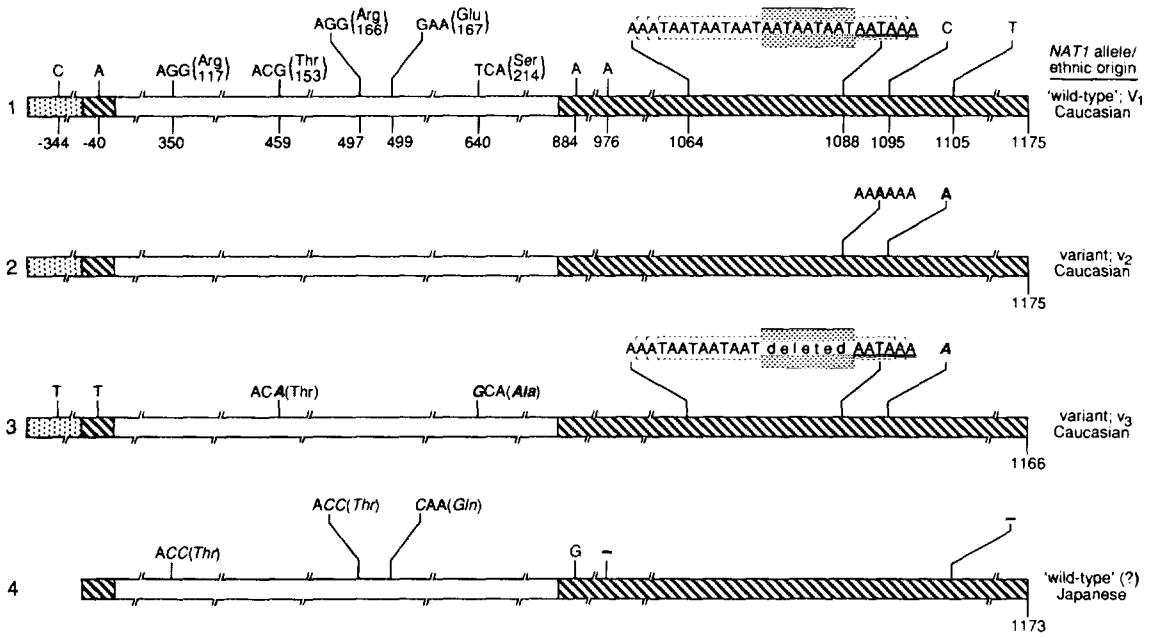

FIG. 6. Genetic heterogeneity of human *NAT1*. The 1.6-kb fragments (not drawn to scale) of Caucasian 'wt' (line 1) and variant (lines 2 and 3) *NAT1* alleles identified in this study are compared to a presumably 'wt' *NAT1* allele from Japanese (5). The various *NAT1* regions are marked as in Fig. 1. A 3' UTR sequence containing the consensus polyadenylation signal (underlined) is depicted on line 1 (nt 1064–1091). The element $(AAT)_3$—highlighted by the shaded frame—is shown as "deleted" from variant v_3 (line 3), but this is intended merely as an example of a potential deletion site. The 26-bp segment from nt 1065 to 1090 consists of eight iterative AAT, ATA, and TAA triplets, giving rise to 18 nonanucleotide combinations [six each for the $(AAT)_3$, $(ATA)_3$, and $(TAA)_3$ motifs] as potential deletion sites (indicated by the dashed lines above and below this segment). Elimination of each of these 9-nt elements results in the same sequence for allele v_3, making it impossible to distinguish the deletion point. Two of the five missense mutations in variant v_3 were at hypermutable CpG dinucleotides [nt −344 and 459; lines 1 and 3 (8)]. Significant differences exist between Caucasian *NAT1* allele V_1 (line 1) and the putative 'wt' allele from Japanese [line 4 (5)]. Of the six nucleotide dissimilarities, five are in the coding exon and involve replacement of two cationic and one anionic residue (line 1) by three uncharged polar residues (line 4). Two deletions in the 3' UTR of the Japanese 'wt' allele are shown with a dash (nt 976 and 1105).

as monomorphic (3–5), is indeed polymorphic. The validity of the observed *NAT1* mutations is documented by the heterozygosities in over 40% of the 12 unrelated individuals (Table 1, penultimate column), and further substantiated by the Mendelian inheritance of the variant alleles (subject 2 is the offspring of subjects 8 and 9; Table 1, last two columns). Moreover, acetylator phenotypes [assessed with 'NAT2-type substrates' (6)] and *NAT2* genotypes were interspersed with *NAT1* genotypes, strengthening the suggestion from catalytic activity experiments (6) that the two NAT genes are independently expressed.

None of the most commonly studied restriction sites was eliminated or created by the mutations in variants v_2 and v_3, indicating that RFLP analysis would have disclosed no banding pattern differences for *NAT1*. In fact, Southern blots of *Kpn*I-, *Bam*HI-, or *Eco*RI-digested DNA from three human livers showed no RFLPs when probed with NAT1 cDNA, whereas a *Kpn*I RFLP was apparent in blots probed with NAT2 cDNA (3). The absence of RFLPs, therefore, by no means signifies structural invariability for a given gene.

The 3' UTR of 'wt' *NAT1* (allele V_1) contains multiple copies of AAT, ATA, and TAA motifs (nt 1065–1090; Fig. 6, line 1), which resemble the 'destabilizing' AT-rich elements in the 3' UTR of several eukaryotic mRNAs with high turnover rates (14). These 'destabilizing' units are known to facilitate mRNA degradation by disrupting association of the poly(A) tract with PABP (14–16), inferring that the AT-rich structure in the 3' UTR of allele V_1 could similarly promote destruction of V_1 mRNA. Variant v_2 mRNA may also be short-lived as a consequence of the mutated polyadenylation signal in allele v_2 (nt 1086–1091; Fig. 6, line 2), since (a) point mutations within the highly conserved AATAAA sequence prevent mRNA cleavage and polyadenylation (17), and (b) nonpolyadenylated mRNAs undergo accelerated degradation in the absence of a stabilizing poly(A)–PABP complex (16). Low levels of 'wt' (V_1) mRNA or variant v_2 mRNA would be accompanied by formation of scant but otherwise normal V_1 or v_2 protein. Two observations, made with tissue preparations of undetermined *NAT1* genotype, lend support to this postulate: hepatic NAT1 mRNA is scarce (3); and immunoreactive NAT1 is undetectable in crude liver cytosol (4) and only barely detectable on Western blots of column fractions with partially purified cytosol possessing

ample activity toward *p*-aminosalicylic acid, even when loaded in an amount five-fold greater than that of NAT2-containing fractions (6). In sharp contrast, the 3′ UTR of *NAT2* is devoid of AT-rich segments (3, 4), hepatic NAT2 mRNA is abundant (3, 9), and immunoreactive NAT2 is readily seen in crude liver cytosol with moderately high sulfamethazine N-acetylation activity (4, 9).

Removal of one-third of the 'destabilizing' AT-rich segment from the 3′ UTR of mutant allele v_3 (Fig. 6, line 3) could result in elevated steady-state levels of v_3 mRNA. On the other hand, upstream and coding region mutations in v_3 may adversely affect the translational efficiency of v_3 mRNA or lead to production of a labile protein, as has been described for two Caucasian *NAT2* variants (9). In any event, deletions from 3′ UTR sequences are not uncommon. Two deletions are seen in the 3′ UTR of 'wt' *NAT1* from Japanese relative to that from Caucasians (Fig. 6, lines 1 and 4), and have also been found in this region of eukaryotic genes and cDNAs encoding two P450s and an array of proteins unrelated to drug metabolism (18).

Human NAT1 and NAT2 are expressed in liver (6), whereas NAT1 is by far the predominant acetylase in mononuclear leukocytes (19). NAT1 has a selectivity for *p*-aminosalicylic and *p*-aminobenzoic acids (6), both of which have traditionally been classified as 'monomorphic substrates' (1–3, 6, 19–21). In this connection, some old and new observations merit consideration. Dissimilarities in *p*-aminosalicylic acid N-acetylation rates had been noted almost 30 years ago by Jenne (21) with partially purified human liver cytosolic NAT preparations, but the significance of this finding was ignored because of the constancy in rates of elimination of this compound by humans *in vivo* (20, 21). A difference in the thermostability of *p*-aminobenzoate *N*-acetylase was later detected in lymphocytes from 39 persons, and a host of criteria favored the conclusion that the differential heat stability most likely reflected a "structural gene difference" (22). Moreover, a population study on *p*-aminobenzoate N-acetylation by whole blood from 200 human subjects revealed a frequency distribution with a tendency toward bimodality (23). More recent investigations have corroborated and extended the *in vitro* findings of Jenne (21) by demonstrating a dramatic variation (more than 25-fold) in *p*-aminosalicylate and *p*-aminobenzoate N-acetylation by cytosol from 39 human autopsy liver specimens (6), as well as a seven-fold variation in rates of *p*-aminobenzoate N-acetylation by the cytosolic fraction of mononuclear leukocytes from 23 individuals of undefined *NAT1* genotype (19). Lastly, and contrary to the earlier *in vivo* results (1, 2, 20, 21), a preliminary study[4] presented after completion of the present work indicates that *p*-aminosalicylate elimination in 130 healthy volunteers, assessed by HPLC measurements of N-acetylated and parent drug in urine, is bimodal. It seems reasonable, therefore, that the profound structural heterogeneity at the human *NAT1* locus described in the present paper could be the genetic basis for the substantial catalytic activity differences seen with *p*-aminosalicylate and *p*-aminobenzoate *in vitro* and *in vivo,* thereby suggesting that human NAT1 participates in an acetylation polymorphism distinct from that typified by isoniazid and sulfamethazine.

REFERENCES

1. Weber, W. W. (1987) The Acetylator Genes and Drug Response, Oxford University Press, New York.
2. Evans, D. A. P. (1989) *Pharmacol. Ther.* **42,** 157–234.
3. Ohsako, S., and Deguchi, T. (1990) *J. Biol. Chem.* **265,** 4630–4634.
4. Blum, M., Grant, D. M., McBride, W., Heim, M., and Meyer, U. A. (1990) *DNA Cell Biol.* **9,** 193–203.
5. Ebisawa, T., and Deguchi, T. (1991) *Biochem. Biophys. Res. Commun.* **177,** 1252–1257.
6. Grant, D. M., Blum, M., Beer, M., and Meyer, U. A. (1991) *Mol. Pharmacol.* **39,** 184–191.
7. Deguchi, T., Mashimo, M., and Suzuki, T. (1990) *J. Biol. Chem.* **265,** 12757–12760.
8. Vatsis, K. P., Martell, K. J., and Weber, W. W. (1991) *Proc. Natl. Acad. Sci. USA* **88,** 6333–6337.
9. Blum, M., Demierre, A., Grant, D. M., Heim, M., and Meyer, U. A. (1991) *Proc. Natl. Acad. Sci. USA* **88,** 5237–5241.
10. Vatsis, K. P., and Weber, W. W. (1991) *Am. J. Hum. Genet.* **49,** 112A.
11. Müllenbach, R., Lagoda, P. J. L., and Welter, C. (1989) *Trends Genet.* **5,** 391.
12. Kilbane, A. J., Silbart, L. K., Manis, M., Beitins, I. Z., and Weber, W. W. (1990) *Clin. Pharmacol. Ther.* **47,** 470–477.
13. Weber, W. W., and Brenner, W. (1974) *Am. J. Hum. Genet.* **26,** 467–473.
14. Shaw, G., and Kamen, R. (1986) *Cell* **46,** 659–667.
15. Bernstein, P., and Ross, J. (1989) *Trends Biochem. Sci.* **14,** 373–377.
16. Jackson, R., and Standart, N. (1990) *Cell* **62,** 15–24.
17. Humphrey, T., and Proudfoot, N. J. (1988) *Trends Genet.* **4,** 243–245.
18. Levitt, R. C. (1991) *Genomics* **11,** 484–489.
19. Cribb, A. E., Grant, D. M., Miller, M. A., and Spielberg, S. P. (1991) *J. Pharmacol. Exp. Ther.* **259,** 1241–1246.
20. Evans, D. A. P. (1963) *Am. J. Med.* **34,** 639–662.
21. Jenne, J. W. (1965) *J. Clin. Invest.* **44,** 1992–2002.
22. McQueen, C. A., and Weber, W. W. (1980) *Biochem. Genet.* **18,** 889–904.
23. Weber, W. W., and Vatsis, K. P. (1993) *Pharmacogenetics,* in press.

[4] Grant, D. M., Vohra, P., Avis, Y., and Ima, A. (1992) Proceedings of the 9th International Symposium on Microsomes and Drug Oxidations, p. 244. Jerusalem, Israel, July 6–9.